frontiers in Marine Science

ORIGINAL RESEARCH
published: 16 March 2022
doi: 10.3389/fmars.2022.836341

Taxonomy and Phylogeny of Two Spirotrichean Ciliates (Alveolata, Protista, and Ciliophora) From a Plateau Saline–Alkaline Lake in Tibet, China, Including Description of a New Species

Farzana Kouser[1,2†], Wenya Song[1,2†], Limin Jiang[1,2†], Wenbao Zhuang[1,2], Congcong Wang[1,2], Tong Wu[1,2] and Xiaozhong Hu[1,2]*

[1] *Key Laboratory of Mariculture, Ministry of Education, College of Fisheries, Ocean University of China, Qingdao, China,*
[2] *Institute of Evolution and Marine Biodiversity, Ocean University of China, Qingdao, China*

OPEN ACCESS

Edited by:
Sandra Pucciarelli, University of Camerino, Italy

Reviewed by:
Santosh Kumar, Zoological Survey of India, India
Xumiao Chen, Institute of Oceanology (CAS), China

***Correspondence:**
Xiaozhong Hu
xiaozhonghu@ouc.edu.cn

† These authors have contributed equally to this work

Specialty section:
This article was submitted to Marine Evolutionary Biology, Biogeography and Species Diversity, a section of the journal Frontiers in Marine Science

Received: *15 December 2021*
Accepted: *31 January 2022*
Published: *16 March 2022*

Citation:
Kouser F, Song W, Jiang L, Zhuang W, Wang C, Wu T and Hu X (2022) Taxonomy and Phylogeny of Two Spirotrichean Ciliates (Alveolata, Protista, and Ciliophora) From a Plateau Saline–Alkaline Lake in Tibet, China, Including Description of a New Species. Front. Mar. Sci. 9:836341. doi: 10.3389/fmars.2022.836341

There are few researches concerning ciliates from "extreme" environments such as plateau salt lakes; nevertheless, such a faunistic survey is of great significance for understanding the diversity and biogeography of these microeukaryotes. In this study, two ciliates, namely, *Hemiurosomoida tibetensis* sp. nov. and *Euplotes euryhalinus* Valbonesi and Luporini, 1990, isolated from Kyêbxang Co, a Tibet Plateau saline-alkaline lake, China, were investigated based on observations of live and silver-stained specimens, and 18S rDNA sequences were analyzed. The new species can be characterized by having a size of 60–95 × 20–40 μm *in vivo*, an elongate elliptical body, colorless cortical granules mainly grouped around cirri and dorsal bristles, about 21 adoral membranelles, 20 cirri on each marginal row, and two macronuclear nodules and two micronuclei. The Chinese population of *E. euryhalinus* corresponds well with the original one. Phylogenetic analyses show that *Hemiurosomoida* is non-monophyletic, *H. tibetensis* sp. nov. has a closer relationship with *H. longa* within this genus, and that *Euplotes euryhalinus* presents a wide geographic distribution. This study first reveals the ciliature, morphogenesis, and rRNA gene sequence data for *H. tibetensis* sp. nov. and the Chinese population of *E. euryhalinus*, which thus increases our knowledge about the diversity of ciliates at high altitudes.

Keywords: biodiversity, ciliates, "extreme" environment, new species, SSU rRNA gene

INTRODUCTION

There are numerous records about ciliated protists (phylum Ciliophora) in "common" biotopes such as freshwater, seawater, and soil (Dragesco and Dragesco-Kernéis, 1986; Carey, 1992; Berger, 2008; Song et al., 2009, 2021; Küppers et al., 2011; Foissner, 2016; Hu et al., 2019; Liu et al., 2021). By contrast, relatively few researches concern ciliates from "extreme" environments (Hu, 2014), such as anoxic ones (Li et al., 2017, 2021), chilly bipolar regions (Xu et al., 2016), hot springs

(Qu et al., 2018), deep-sea hydrothermal vents (Small and Lynn, 1985; Kouris et al., 2007), alkaline water (Odhiambo et al., 2013), and hypersaline habitats (Oren, 2002; Foissner, 2012; Qu et al., 2020). These limited number of studies have revealed a high level of speciation and structural divergence in ciliates as demonstrated by continual discoveries of novel taxa. Among these abnormal conditions, plateau, especially saline-alkaline lakes are extremely under-sampled mainly owing to hypoxic and hypotension (Shen, 1983), which hampers our understanding of the diversity and phylogeny as well as distribution of ciliates. To reveal the species composition of ciliates, we surveyed a saline-alkaline lake in Tibet, China, and documented two species in this article.

Oxytrichidae Ehrenberg, 1838, as one of the most diverse and complex families in the Ciliophora, is almost ubiquitous and includes more than 40 genera so far (Berger, 1999; Singh and Kamra, 2013; Shao et al., 2015, 2019; Foissner, 2016; Jung et al., 2017; Kaur et al., 2019; Xu et al., 2020; Luo et al., 2021). More than 30% of the recognized genera show low species richness (Berger, 1999; Kumar et al., 2014, 2017; Kumar and Foissner, 2017; Kabir et al., 2020). Being an example, *Hemiurosomoida* was erected by Singh and Kamra, with *H. longa* (basionym: *Oxytricha longa* Gelei and Szabados, 1950) designated as the type species (Singh and Kamra, 2015). Very recently, *H. warreni* was added to the genus (Chen et al., 2021). Considering its unique somatic ciliature, one species found in this survey represents an unknown *Hemiurosomoida*.

Euplotes Ehrenberg, 1830, is a speciose ciliate genus and several taxonomists have recognized more important characters for species delineation (Tuffrau, 1960; Borror, 1972; Carter, 1972). Curds (1975) provided the most recent taxonomic revision (Berger, 2011). With the addition of new members recently (Jiang et al., 2010a,b; Pan et al., 2012; Chen et al., 2013; Fotedar et al., 2016; Syberg-Olsen et al., 2016; Ivalji et al., 2020; Lian et al., 2020, 2021; Abraham et al., 2021), so far more than 160 species and sub-species have been included in *Euplotes* s. l (Berger, 2001). However, the identification of *Euplotes* species remains difficult even though many species have been investigated using a range of modern methods for (1) remarkable intraspecific variation of diagnostic characters even within clonal cultures; (2) poor original report and self-contradiction of re-descriptions in certain common species (Kahl, 1930–1935; Burkovsky, 1970; Carter, 1972; Agatha et al., 1993; Petz et al., 1995; Song and Wilbert, 2002). *Euplotes euryhalinus* was first reported by Valbonesi and Luporini (1990) from cold water in Antarctica, with a pattern of dorsal argyrome and ciliature under protargol-staining and electron microscopy supplied, but lacking morphological information *in vivo* and corresponding molecular data. In this study, it was rediscovered, which provided a good chance to supplement the description of the species.

MATERIALS AND METHODS

Sample Collection and Identification

Samples were collected from the Kyêbxang Co (32°27′29″N; 89°59′35″E), Tibet (**Supplementary Figures 1A–C**) using the polyurethane foam unit (PFU) method (Hu and Kusuoka, 2015). The Kyêbxang Co is a plateau saline-alkaline lake at an altitude of approximately 4,660 m above sea level. The PFUs were placed in the lake at a depth of 50 cm for approximately 2 months (from August to October 2019) as artificial substrata to colonize ciliates. The water temperature, salinity, and pH are 8.81°C, 41.39‰, and 10.13, respectively, when the PFUs were collected. The sponges and habitat water were then transported to the laboratory for further treatment. Isolated specimens were maintained in the laboratory for approximately 1 week as raw or uni-protistan cultures.

Living cells were observed with a light microscope equipped with differential interference contrast (100–1,000 ×). The protargol staining method was used to reveal the ciliature and nuclear apparatus (Wilbert, 1975). The Chatton–Lwoff silver nitrate impregnation was applied to reveal the silverline system (Foissner, 2014). The DAPI silver samples were incubated with 50% formalin solution (1:1 v/v) at room temperature for 1 min and stained with DAPI solution at 1.25 μg/ml final concentration to visualize the nuclei (Gong et al., 2020). Counts and measurements of stained specimens were performed at a magnification of × 1,250. Drawings of living cells were produced based on freehand sketches and photomicrographs, and drawings of silver-stained specimens were made with the help of a camera lucida.

DNA Extraction, PCR Amplification, and Sequencing

For each species, a single cell was picked directly from the original sample and washed five times using autoclaved ultrapure water before DNA extraction Genomic DNA was extracted using DNeasy Blood and Tissue Kit (QIAGEN, Hilden, Germany), following the manufacturer's instructions. Primers 18S-F (5′-AAC CTG GTT GAT CCT GCC AGT-3′) and 18S-R (5′-TGA TCC TTC TGC AGG TTC ACC TAC-3′) were used for SSU rDNA amplification (Medlin et al., 1988). To minimize the possibility of PCR amplification errors, Q5® Hot Start High-Fidelity DNA Polymerase (New England BioLabs, United States) was used. The PCR amplification protocol followed was as follows: 30 s initial denaturation (98°C), 35 cycles of 10 s at 98°C, 30 s at 69°C, 1 min at 72°C, and a final 2 min at 72°C. Sequencing was performed bidirectionally by the Tsingke Biological Technology Company (Qingdao, China).

Phylogenetic Analyses

Besides the two newly obtained sequences, further 109 sequences used in the present phylogenetic analyses were downloaded from GenBank. *Novistrombidium orientale* (FJ422988) and *Strombidium apolatum* (DQ662848) were selected as outgroups. Sequence alignments were performed online using the MUSCLE software package on the European Bioinformatics Institute web server.[1] The resulting alignment was checked and edited manually, leading to a matrix with 2,224 positions.

Maximum likelihood (ML) analysis with 1,000 bootstrap replicates was performed to estimate the reliability of internal

[1]http://www.ebi.ac.uk/Tools/msa/muscle/

branches using RAxML-HPC2 on XSEDE v.8.2.10, with the GTR + I + G model provided on the online server CIPRES Science Gateway (Stamatakis, 2014). Bayesian inference (BI) analysis was run using MrBayes v.3.2.6 on XSEDE on the CIPRES Science Gateway with the GTR + I + G model (selected using MrModeltest v.2.2) (Nylander, 2004). Markov Chain Monte Carlo (MCMC) simulations were then run with two sets of four chains using the default settings. MCMC simulations were then run with two sets of four chains using the default settings. The chain length for the analysis was 10,000,000 generations with trees sampled every 100 generations. The first 10% of trees were discarded as burn-in. The remaining trees were used to calculate posterior probabilities by a majority rule consensus. MEGA v.6.0 (Kumar et al., 2016) was used to visualize tree topology. Systematic and terminology classification follow Curds (1975) and Shao et al. (2015).

The unbiased (AU) test (Shimodaira, 2002) was used to assess phylogenetic relationships among different taxa within *Hemiurosomoida*. One constrained and unconstrained ML tree was generated by RAxML v.8.2.10 (Stamatakis, 2014) with the enforced constraints. The site-wise likelihood values were calculated by RAxML v.8.2.10 (Stamatakis, 2014) and then compared in CONSEL (Shimodaira and Hasegawa, 2001). Additionally, the SSU rRNA gene sequence comparisons of species (*Hemiurosomoida* species and *Parakahliella macrostoma*) in the present study were performed by BioEdit version 7.0.5.2 (Hall, 1999).

RESULTS

ZooBank Registration

Present work: urn:lsid:zoobank.org:pub:C13AC67A-2F47-4879-9D90-3E45F67D33C6.

Hemiurosomoida tibetensis sp. nov.: urn:lsid:zoobank.org:act:19F9C547-51C8-4F0C-83C9-9681ACBF0EC7.

Taxonomy and Description of *Hemiurosomoida tibetensis* sp. nov.

Spirotrichea Bütschli, 1889
Hypotrichia Stein, 1859
Dorsomarginalia Berger, 2006
Oxytrichidae Ehrenberg, 1838
Hemiurosomoida Singh and Kamra, 2015
Hemiurosomoida tibetensis sp. nov.

Diagnosis

Size *in vivo* 60–95 × 20–40 μm; body flexible, elongate elliptical; cortical granules spherical and colorless, mainly distributed along cirri on the ventral side and around dorsal cilia, and between dorsal kineties; two macronuclear nodules, each closely associated with a micronucleus; contractile vacuole located at anterior 40% of cell length near left margin; adoral zone approximately 25–30% of cell length, composed of 17–24 membranelles; marginal rows not confluent posteriorly, each with 20 cirri on average; dorsal kineties 1–3 with about 7–12, 8–12, and 8–12 bristles, respectively, and two caudal cirri at the posterior end of dorsal kineties 1 and 2.

Type Locality

Kyêbxang Co (32°27′29″N; 89°59′35″ E), Tibet, China. The water temperature, salinity, and pH are 8.81°C, 41.39‰, and 10.13, respectively.

Type Materials

Two protargol-stained slides including the holotype (**Figures 1B,C**) and paratypes were deposited in the Laboratory of Protozoology, Ocean University of China, Qingdao, China.

Description

Body about 60–95 × 20–40 μm *in vivo*, on average 70 × 35 μm in stained specimens. Shape almost constant, usually elongate elliptical with anterior and posterior ends broadly rounded (**Figures 1A**, **2A–D**), the ratio of length to width about 2.2:1 after protargol staining. Cell flexible and non-contractile. Cortical granules colorless (*ca.* 0.6–1.0 μm), spherical, grouped along cirri on the ventral side and around dorsal cilia, and between dorsal kineties (**Figures 1D,E**, **2E**). Cytoplasm is colorless, containing few to many lipid droplets (*ca.* 0.5–3.0 μm across) and food vacuoles (*ca.* 1.5–5.0 μm) (**Figure 2E**). Contractile vacuole located at anterior two-fifth of body length near the left margin, about 7 μm across (**Figures 1A**, **2C**). Two oval macronuclear nodules, about 10–12 × 10 μm *in vivo*, closely spaced nearly in the middle portion slightly left of midline, each attached by a spherical micronucleus (**Figures 1C**, **2F,G**). Locomotion is by crawling slowly over the substrate.

Adoral zone occupying approximately 25–30% of cell length, on average 32% of body length after protargol staining; composed of 17–24 membranelles (**Figures 1A,B 2A–D,H** and **Table 1**). Cilia of apical membranelles up to 14 μm long *in vivo*. Undulating membranes in *Stylonychia* pattern, paroral membrane and endoral membrane straight and parallel to each other, with almost equal length; the endoral ahead of the paroral (**Figures 1B**, **2H,I**).

The cirral pattern constant, and the number of cirri almost invariable. Three frontal cirri slightly enlarged, the right one behind the distal end of the adoral zone. Buccal cirrus right of the anterior end of endoral membrane. Four frontoventral cirri arranged in a V-shaped pattern, cirrus III/2 at the same level of cirrus VI/3. Four transverse cirri J-shaped. Three postoral ventral cirri closely positioned, near the proximal end of the adoral zone. Two pretransverse cirri, the left one ahead of cirrus III/1, the right one just anterior to cirrus VI/1. One marginal row on each side of the cell, non-confluent posteriorly, almost equal in the number of cirri, the left row commencing at the level of left of the proximal portion of the buccal field and extending to the rear end of the cell, right one starting at right of cirrus IV/3 (**Figures 1B**, **2H**). Transverse cirri about 14–16 μm long *in vivo*, all of them protruding beyond the rear end of the cell (**Figures 1A**, **2H**). Invariably, four dorsal kineties including one dorsomarginal row (dorsal kinety 4) with conspicuously long dorsal cilia, approximately 4.5–5.0 μm long *in vivo*. Dorsal kineties 1–3 almost throughout the

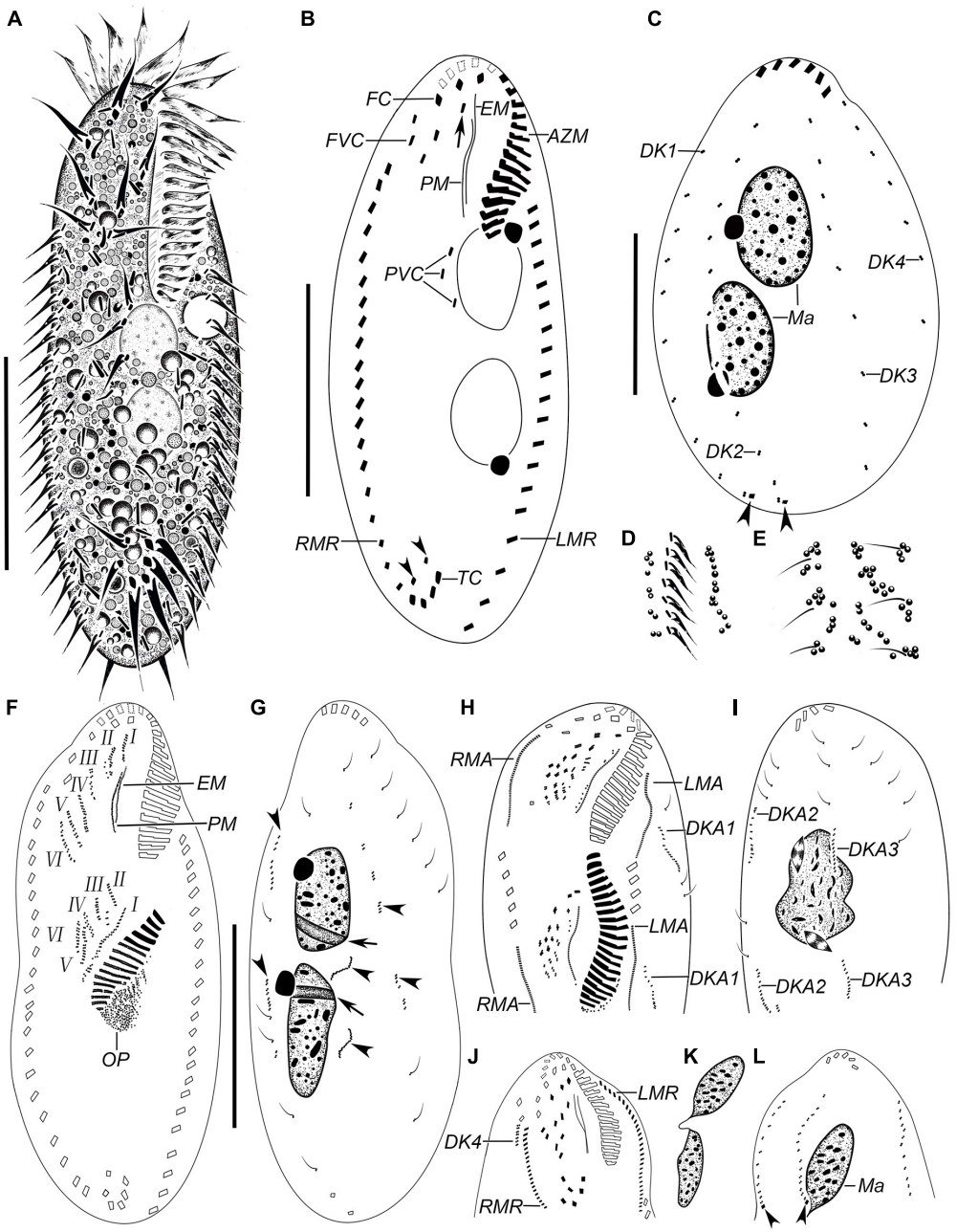

FIGURE 1 | *Hemiurosomoida tibetensis* sp. nov. *in vivo* **(A,D,E)** and after protargol staining **(B,C,F–L)**. **(A)** Ventral view of a representative individual. **(B)** Ventral view of the holotype, showing ciliature and nuclear apparatus, arrowheads in **(B)** indicate two pretransverse ventral cirri, arrow indicates buccal cirrus. **(C)** Dorsal kineties and nuclear apparatus, arrowheads mark caudal cirri. **(D)** Part of ventral view, to show the arrangement of cortical granules. **(E)** Part of dorsal view, to show the arrangement of cortical granules. **(F,G)** Ventral **(F)** and dorsal **(G)** view of the same early divider, showing the development of opisthe's oral primordium and cirral anlagen; arrows indicate replication bands, arrowheads mark dorsal kineties anlagen. **(H,I)** Part of ventral **(H)** and dorsal **(I)** view of the same middle divider. Arrow in **(H)** and arrowhead in **(I)** mark buccal and paroral membrane, respectively. **(J,L)** Ventral **(J)** and dorsal **(L)** of the same proter at late morphogenesis stage, showing the ciliature, arrowheads indicate caudal cirri. **(K)** Two macronuclear nodules of the same proter as in figures **(J,L)**. AZM, adoral zone of membranelles; DK1–4, dorsal kineties 1–4; DKA1–3, dorsal kinety anlagen 1–3; EM, endoral membrane; FC, frontal cirri; FVC, frontoventral cirri; I–VI, frontal-ventral-transverse anlagen 1–VI; LMA, anlage of left marginal row; LMR, left marginal row; Ma, macronucleus; Mi, micronucleus; PM, paroral membrane; PVC postoral ventral cirri; RMA, anlage of right marginal row; RMR, right marginal row; TC, transverse cirri. Bars, 30 μm.

entire body length, composed of on average 9, 10, and 10 dikinetids, respectively. Dorsal kinety 4 with about 7 dikinetids, commencing at the anterior end of the cell and terminating at mid-body (**Figure 2C**). Two caudal cirri, about 10–12 μm *in vivo*, one each at the posterior end of dorsal kineties 1 and 2 (**Figures 1C**, **2J**).

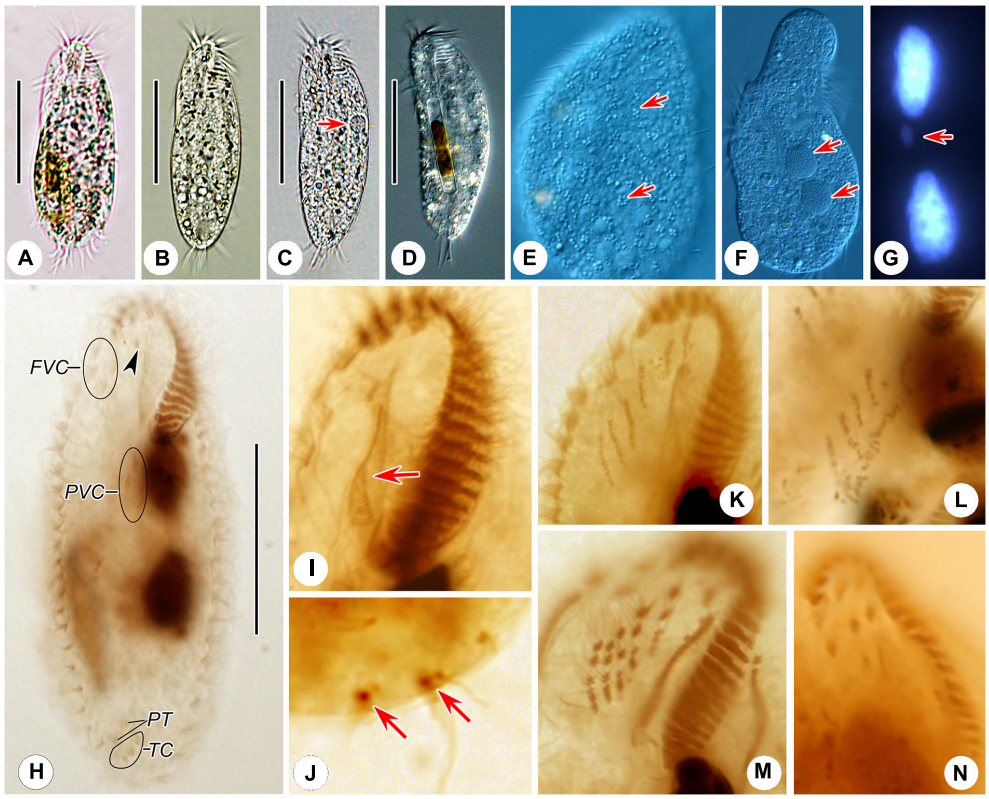

FIGURE 2 | Photomicrographs of *Hemiurosomoida tibetensis* sp. nov. *in vivo* **(A–F)**, after DAPI staining **(G)** and protargol **(H–N)** staining. **(A–D)** Ventral view of different cells, showing variation in body shapes and contractile vacuole (arrow). **(E)** Dorsal view, showing the arrangement of cortical granules (arrows). **(F)** Two spherical macronuclear nodules (arrows). **(G)** Two macronuclear nodules and one ellipsoid micronucleus (arrow). **(H)** Ventral infraciliature and nuclear apparatus of the holotype, arrowhead indicates buccal cirrus. **(I)** Ventral view of infraciliature of the anterior portion of a specimen, arrow shows paroral membrane. **(J)** Two caudal cirri (arrows). **(K,L)** Ventral views, show the newly formed frontal-ventral-transverse cirral anlagen in both proter **(K)** and opisthe **(L)**. **(M,N)** Ventral views, showing the newly formed cirri in the proter. FVC, frontoventral cirri; PT, pretransverse ventral cirri; PVC postoral ventral cirri; TC, transverse cirri. Bars, 40 μm.

Note on Morphogenesis

In the opisthe, oral primordium lengthens and differentiates into new membranelles in a posteriad direction (**Figures 1F,H**); at the same time, undulating membranes (UM) anlage (I) is formed as a streak at the right of the oral primordium, which will split into the paroral and endoral membranes and produce the left frontal cirrus at its anterior end later (**Figure 1H**). In the proter, the parental adoral zone of membranelles remains entirely unchanged; however, the parental undulating membranes dedifferentiate from their anterior portion and gradually produce UM-anlage (**Figures 1F**, **2I**), developing in the same way as in the opisthe. In a middle divider, five streaks of the frontal–ventral–transverse cirral anlagen (FVTA II–VI) form to the right of the UMA in both proter and opisthe, separately (**Figures 1F**, **2K,L**); however, it remains obscure if these anlagens are derived from primary primordia or not. At this time, cirri III/2, IV/2, IV/3, V/3, and V/4 disappear. Later, these streaks fragment and form 16 new cirri in a 2: 3: 3: 4: 4 pattern from left to right (**Figures 1H,J**, **2M,N**).

Both marginal row anlagens develop within the parental rows in both opisthe and proter, and later than the origin of FVTA (**Figure 1H**). Then, all marginal cirral anlagens enlarge and generate new cirri while the parental structures gradually disintegrate and disappear (**Figure 1J**). In the same way, two sets of dorsal kinety anlagens (DKA) 1–3 occur intrakinetally (**Figures 1D,G–I**). The DKA 4 is formed to the right of the right marginal row and then develops into the short dorsomarginal kinety (**Figure 1J**). One caudal cirrus is formed at the posterior end of the new DKA 1 and 2, respectively (**Figure 1L**). While the DKA 1–4 proliferate and extend at both ends, the parental bristles gradually become resorbed.

One replication band was seen in each macronuclear nodule (**Figure 1G**), then two nodules completely fuse into a single mass, which was then divided two times for both proter and opisthe in the late stage (**Figures 1I,K**).

Taxonomy and Morphological Description of *Euplotes euryhalinus* Valbonesi and Luporini, 1990

Euplotia Jankowski, 1979
Euplotida Small and Lynn, 1985
Euplotidae Ehrenberg, 1838
Euplotes Ehrenberg, 1830
Euplotes euryhalinus Valbonesi and Luporini, 1990

TABLE 1 | Morphometric data on *Hemiurosomoida tibetensis* sp. nov.

Characters	Min	Max	Mean	*M*	*SD*	CV	n
Body length	53	86	71.2	75	10.3	14.5	21
Body width	20	48	33.5	32	6.3	18.9	21
Length of buccal field	15	27	23	24	3.5	15.3	21
Buccal field length:body length, ratio (%)	26	40	33	32.5	3.1	34.0	21
Number of adoral membranelles	17	24	20.7	20	1.6	7.6	21
Number of buccal cirrus	1	1	1	1	0	0	21
Number of frontal cirri	3	3	3	3	0	0	21
Number of frontoventral cirri	4	4	4	4	0	0	21
Number of postoral ventral cirri	3	3	3	3	0	0	21
Number of pretransverse ventral cirri	2	2	2	2	0	0	21
Number of transverse cirri	4	4	4	4	0	0	21
Number of left marginal cirri	16	23	19.7	19.5	2.0	10.4	16
Number of right marginal cirri	16	23	20.1	20.0	1.6	8.1	16
Number of caudal cirri	2	2	2	2.0	0	0	16
Number of dorsal kineties	4	4	4	4	0	0	21
Number of dikinetids in DK1	7	12	9.3	9.0	1.6	16.6	10
Number of dikinetids in DK2	8	12	10.1	10.0	1.3	129	10
Number of dikinetids in DK3	8	12	9.7	9.0	1.6	11.9	10
Number of dikinetids in DK4	5	10	7.2	7.0	2.0	28.1	10
Total number of dikinetids	21	43	32	34.5	5.8	18.2	10
Number of macronuclear nodule	2	2	2	2	0	0	21
Number of micronucleus	2	2	2	2	0	0	21
Anterior macronuclear nodule, length	11	17	14.2	14.0	1.9	13.5	16
Anterior macronuclear nodule, width	6	11	8.3	8.0	1.3	15.7	16
Posterior macronuclear nodule, length	12	21	15.4	14.0	2.7	17.5	16
Posterior macronuclear nodule, width	6	11	8.2	8.0	1.2	15.0	16
Distance between two macronuclear nodule	2	6.7	3.8	3.4	1.3	34.0	16

All data are based on protargol-stained specimens. Measurements in μm. CV, coefficient of variation in%; DK, dorsal kinety; M, median; Max, maximum; Mean, arithmetic mean; Min, minimum; n, number of cells measured. SD, standard deviation.

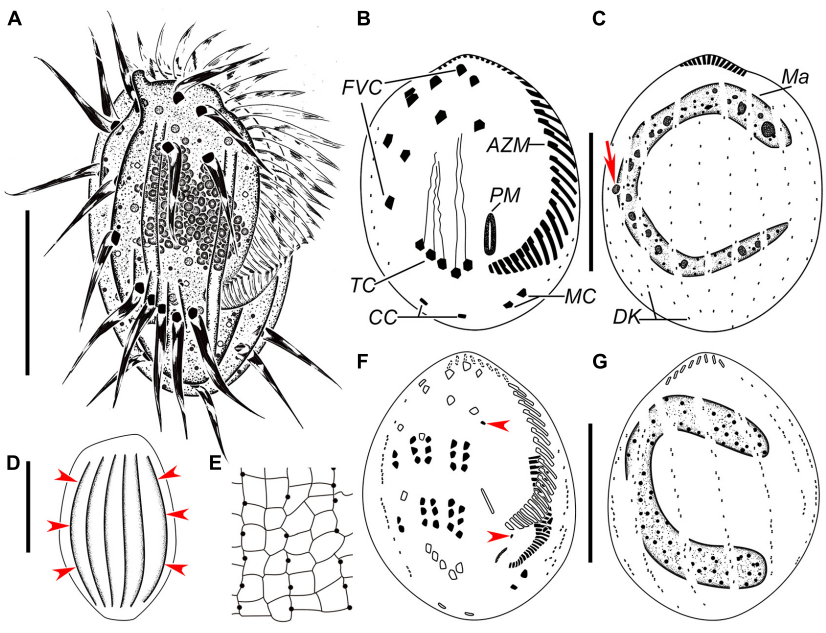

FIGURE 3 | *Euplotes euryhalinus in vivo* **(A,D)**, after protargol **(B,C,F,G)** and silver nitrate **(E)** staining. **(A)** Ventral view of a representative individual. **(B,C)** Infraciliature of ventral **(B)** and dorsal **(C)** sides of the same specimens, arrow in **(C)** marks the micronucleus. **(D)** Dorsal view, to show the conspicuous ridges (arrowheads). **(E)** Part of silverline system on the dorsal side. **(F,G)** Infraciliature of ventral **(F)** and dorsal **(G)** sides of the same middle divider. AZM, adoral zone of membranelles; CC, caudal cirri; FVC, frontoventral cirri; Ma, macronucleus; MC, marginal cirri; PM, paroral membrane; TC, transverse cirri. Bars, 25 μm.

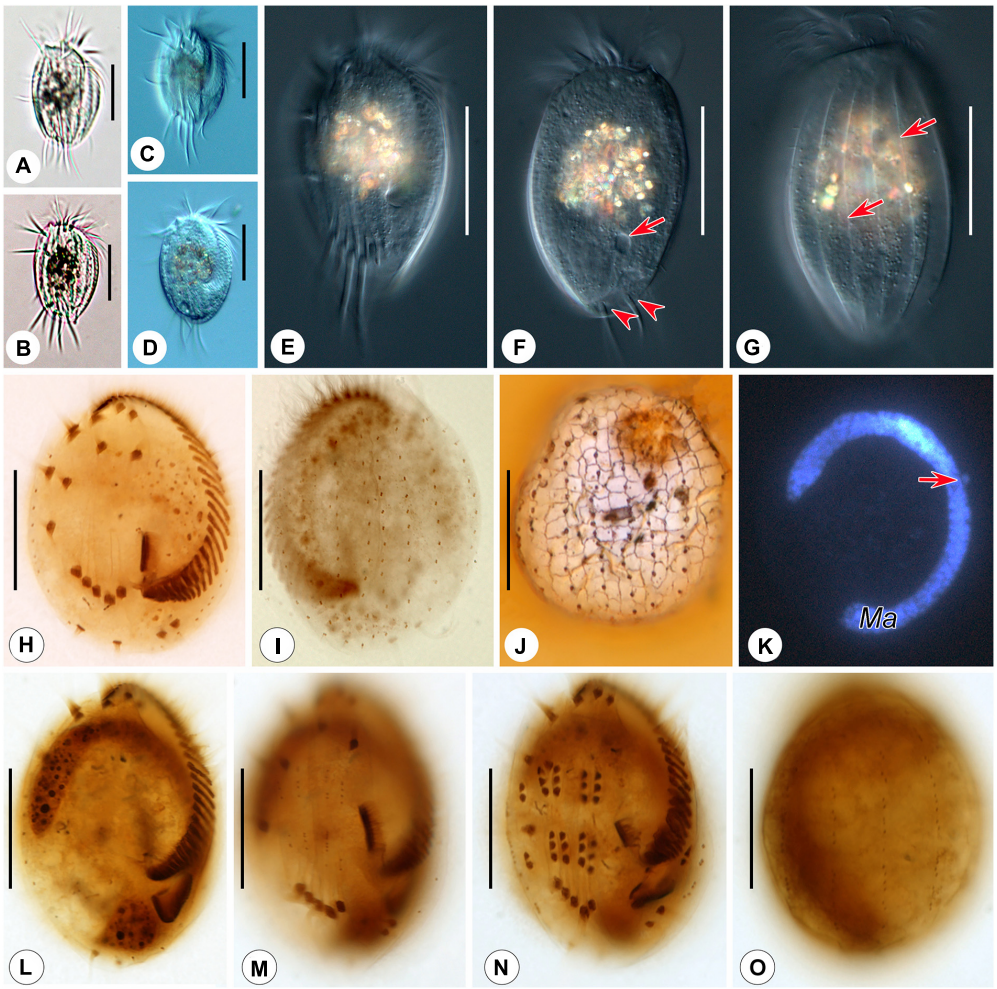

FIGURE 4 | Photomicrographs of *Euplotes euryhalinus in vivo* **(A–G)**, after protargol **(H,I,L–O)**, silver nitrate **(J)**, and DAPI staining **(K)**. **(A–C)** Ventral views of different cells, showing variation in body shape. **(D)** Ventral view, showing contractile vacuole. **(E)** Ventral view, showing conspicuous ridges. **(F,G)** Dorsal view, showing contractile vacuole (arrow in **F**), caudal cirri (arrowheads), and the dominant dorsal ridges (arrows in **G**). **(H,I)** Ciliature of ventral **(H)** and dorsal **(I)** sides of the same specimen. **(J)** Silverline system on the dorsal side. **(K)** C-shaped macronucleus and micronucleus (arrow). **(L,M)** Ventral view of the same early divider, showing oral primordium in opisthe and cirral anlagen. **(N,O)** Ventral **(N)** and dorsal **(O)** view of the same middle divider, showing the development of oral primordium, cirral, and dorsal anlagen. Bars, 25 μm.

Description

Cell size about 45–65 μm × 25–40 μm *in vivo*. Body asymmetrically oval with an anterior portion slightly wider than the posterior portion, and a distinct projection at the right side (**Figures 3A**, **4A–D,F**). Buccal field approximately 75% of cell length. On the ventral side, three long ridges extending posteriorly to the transverse cirri accompanied by short ridges between; on the dorsal side, six conspicuous ridges almost extending the entire cell length (**Figures 3A,D**, **4A–C,E,G**). Dorsal cilia about 1.5 μm long *in vivo*. Cytoplasm colorless, transparent at the marginal area, but opaque in the central part where numerous crystals (2–4 μm) are grouped. Contractile vacuole (?) located dorsally at the level of the rightmost transverse cirri, about 3–4 μm across; its pulsating not observed (**Figure 4F**). Macronucleus consistently C-shaped, with one micronucleus attached to the macronucleus in the middle portion (**Figures 3C**, **4K**). Locomotion typically by moderately fast crawling or incessant jerking on the substrate.

Adoral zone composed of 24–36 membranelles (**Figures 3A,B**, **4H** and **Table 2**). Paroral membrane small, lying under buccal lip (**Figures 3B**, **4H**). Constantly ten frontoventral cirri with cilia about 15 μm long; five transverse cirri, cilia of which are about 20–22 μm long; two caudal cirri caudally positioned and two marginal cirri at the left posterior margin, cilia 11–15 μm in length (**Figures 3A,B**, **4F,H**). A total of 10 or 11 dorsal kineties composed of dikinetids each; the leftmost one with 2–4 dikinetids, located ventrally near the left margin; both the middle and rightmost one with on average 11 dikinetids each (**Figures 3B,C**, **4I** and **Table 2**). The dorsal silverline system double-*eurystomus* pattern (**Figures 3E**, **4J**).

TABLE 2 | Morphometric data on *Euplotes euryhalinus* (Valbonesi and Luporini, 1990).

Characters	Min	Max	Mean	*M*	*SD*	CV	n
Body length	43	60	52.4	53	13.7	26.2	15
Body width	33	50	39.8	39	4.7	11.7	15
Length of buccal field	31	46	40.5	42	4.4	10.8	15
Number of adoral membranelles	24	36	29	29	2.7	9.3	15
Length of paroral membrane	5	10	6.9	7	1.4	19.8	15
Number of frontoventral cirri	10	10	10	10	0	0	15
Number of marginal cirri	2	2	2	2	0	0	15
Number of caudal cirri	2	2	2	2	0	0	15
Number of dorsal kineties	10	11	10.4	10.0	0.5	4.7	10
Number of dikinetids in middle DK	10	13	11.3	11.0	0.9	7.7	10
Number of dikinetids in leftmost DK	2	4	2.6	2.0	0.7	26.0	10
Number of dikinetids in rightmost DK	9	13	11.4	12.0	1.6	13.7	10
Number of transverse cirri	5	5	5	5	0	0	15

All data are based on protargol-stained specimens. Measurements in μm. CV, coefficient of variation in%; DK, dorsal kinety; M, median; Max, maximum; Mean, arithmetic mean; Min, minimum; n, number of cells measured; SD, standard deviation.

Note on Morphogenesis

Only two stages were observed. In an early middle divider, two groups of frontal–ventral–transverse cirral anlagens, each composed of four streaks of basal bodies, appear to the right of the buccal area and between frontoventral cirri and transverse cirri (**Figure 4M**); meanwhile, the opisthe's oral primordium is formed in a subpellicular pouch posterior to the proximal membranelles (**Figure 4L**). In a middle divider, the oral primordium develops into a new adoral zone of membranelles and paroral membrane in the opisthe; five cirral anlagens (II–VI) in either proter or opisthe give rise to cirri in a 3: 3: 3: 3: 2 pattern from left to right; two left marginal cirri and one frontoventral cirrus are formed *de novo*; new anlagens for dorsal kineties occur intrakinetally at two levels (**Figures 3F,G**, **4N,O**). The parental adoral zone of membranelles remains unchanged at these two stages.

18S rRNA Gene Sequence and Phylogeny

The two new SSU rRNA gene sequences obtained in this study were deposited in GenBank. Their lengths, GC contents, and accession numbers are as follows: *Hemiurosomoida tibetensis* sp. nov., 1,730 bp, 45.55%, MZ457562; *Euplotes euryhalinus*, 1,825 bp, 43.71%, MZ457561.

The ML and BI analyses of the SSU rRNA gene sequences generated phylogenetic trees with similar topologies. Therefore, only the ML tree is shown here with support values from both algorithms (**Figure 5**). The new species groups with six populations of *Hemiurosomaida longa* with strong support (ML 91%, BI 1.00), forming a sister clade to the clade formed by *Parakahliella macrostoma* (MH393767) and *Hemiurosomaida warreni* (MT448250) with weak support in ML analysis (60%) and high support in BI analysis (0.99). *Hemiurosomoida tibetensis* sp. nov. differs from *Hemiurosomoida longa* and *Hemiurosomoida warreni* by 46–89 and 42 unmatched nucleotides (94.6–97.2 and 97.4% in sequence identity), respectively. and it differs from *Parakahliella macrostoma* by 46 nucleotides (97.2% in sequence identity) (**Figure 6**). Furthermore, the monophyly of the genus *Hemiurosomaida* is not rejected by the AU test (loglikelihood: –21292.517698, AU value: 0.253). The Tibet population of *Euplotes euryhalinus* clusters into a clade including four other populations of this species (MW369533, EF094967, KP297368, JF903799, JF903800), *Eulpotes indica* (MN038061) and *Euplotes magnicirratus* (AJ549209) with strong to full support, being sister to the *Euplotes* cf. *antarcticus* (FJ998023) + *Euplotes trisulcatus* (EF690810) clade with low to nearly full support (ML 68%, BI 0.99).

DISCUSSION

Comparison of *Hemiurosomoida tibetensis* sp. nov. With Related Species

Hemiurosomoida Singh and Kamra, 2015, was a recently erected genus with reduced transverse cirri, the lack of dorsal kinety 3 fragmentation, and two caudal cirri at the posterior end of dorsal kineties 1 and 2. The newly isolated form matches diagnosed characteristics of the genus but cannot be assigned to any one of two known congeners, namely, *H. longa* and *H. warreni* (Chen et al., 2021), so we named it *H. tibetensis* sp. nov.

Hemiurosomoida longa was first described as *Oxytricha longa* Gelei and Szabados, 1950, and then redefined by Singh and Kamra (2015) based on a few descriptions by Gelei and Szabados (1950) and Ganner et al. (1986, 1987) as well as an Indian population by themselves. It is very similar to *Hemiurosomoida tibetensis* sp. nov., especially in body size and most aspects of ciliature; however, it differs from the latter mainly by the lack of cortical granules (vs. apparently present). The SSU rRNA gene sequence of *Hemiurosomoida longa* isolate (JX893371) with morphological information supplied differs from that of *Hemiurosomoida tibetensis* sp. nov. by 46 nucleotides, which also support the separation of both forms at the species level (**Figure 6**). The other five populations of *H. longa* (MG994998, KY852451, KY912033, AF164125, and AF508763) lack morphological data; of them, the Indian population differs from the remaining populations by 10–51 nucleotides. Compared

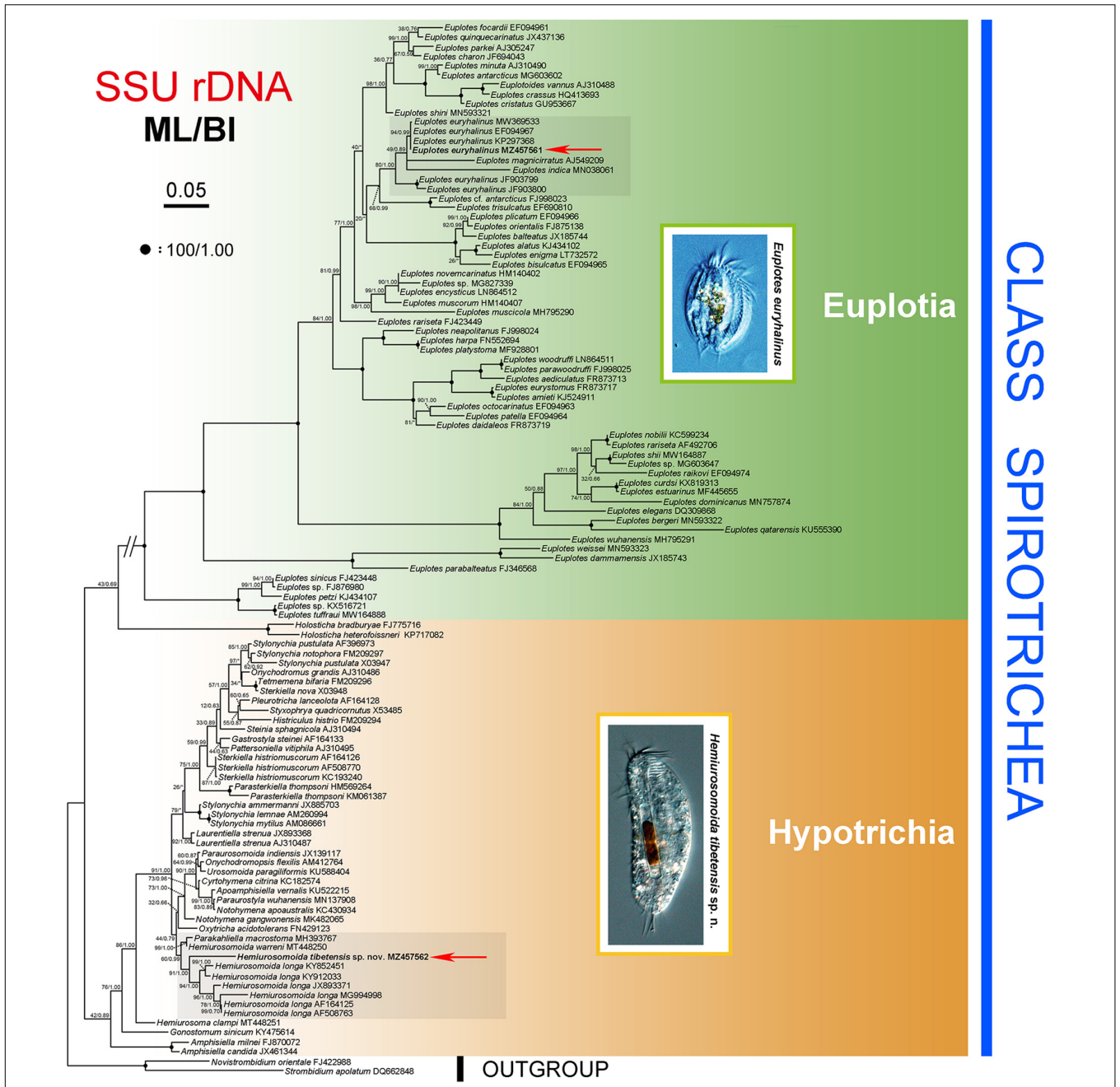

FIGURE 5 | Phylogenetic tree inferred from SSU rRNA gene sequences, revealing the phylogenetic position of *Hemiurosomoida tibetensis* sp. nov. and *Euplotes euryhalinus* (in bold). Numbers near nodes denote maximum likelihood (ML) bootstrap values and Bayesian inference (BI) posterior probabilities, respectively. The scale bar corresponds to five expected substitutions per 100 sites.

with other oxytrichs, *H. longa* indeed presents relatively high SSU rDNA sequence divergence among populations (Li et al., 2018; Luo et al., 2021; Wang et al., 2021), which may infer that cryptic species exist.

Hemiurosomoida warreni can be easily separated from *Hemiurosomoida tibetensis* sp. nov. by the number of macronuclear nodules (4–8 vs. 2), larger body size (110–145 × 30–40 μm vs. 60–95 × 20–40 μm), less transverse cirri (3 vs. 4), and different habitat (soil vs. saline lake) (Chen et al., 2021).

Identification of Tibet Population of *Euplotes euryhalinus*

Euplotes euryhalinus was first reported based on an Antarctic population by Valbonesi and Luporini (1990). Our isolate corresponds well with the original description by the oval body

	1	2	3	4	5	6	7	8	9
1 *H. tibetensis* sp. nov. MZ457562	-	50	52	46	51	51	89	42	46
2 *H. longa* AF164125	96.9%	-	2	10	22	24	43	34	38
3 *H. longa* AF508763	96.8%	99.8%	-	12	24	26	44	36	40
4 *H. longa* JX893371	97.2%	99.3%	99.2%	-	24	24	51	30	34
5 *H. longa* KY852451	96.8%	98.6%	98.5%	98.5%	-	10	59	28	32
6 *H. longa* KY912033	96.8%	98.5%	98.4%	98.5%	99.3%	-	61	26	30
7 *H. longa* MG994998	94.6%	97.4%	97.3%	96.9%	96.4%	96.3%	-	71	75
8 *H. warreni* MT448250	97.4%	97.9%	97.8%	98.1%	98.2%	98.4%	95.7%	-	4
9 *P. macrostoma* MH393767	97.2%	97.6%	97.5%	97.9%	98.0%	98.1%	95.4%	99.7%	-

FIGURE 6 | Nucleotide comparison among populations of *Hemiurosomoida* species and *Parakahliella macrostoma*, based on SSU rRNA gene sequences. A matrix showing the percentage of sequence identity (below the diagonal) and the number of unmatched nucleotides (above the diagonal).

shape, C-shaped macronucleus with one micronucleus situated anteriorly, basic ciliature (constantly ten frontoventral, and five transverse cirri as well as 11 dorsal kineties), and the dorsal silverline system of the "double" type. In the original description, Valbonesi and Luporini (1990) mentioned the presence of four (more occasionally five) caudal cirri, some of which are marginal cirri according to their position. One different characteristic that should be noticed is that there are six prominent ridges on the ventral surface and inconspicuous ridges on dorsal sides in the original population (vs. six conspicuous ridges visible on dorsal sides in our population). According to our observation, they are inconspicuous in bright field microscopy but distinct in differential interference contrast microscopy, and Valbonesi and Luporini (1990) probably overlooked them. Thus, we consider the two populations to be conspecific.

Phylogenetic Analyses

Berger (2006) established the Dorsomarginalia for hypotrichs with dorsomarginal kinety. As a representative, Oxytrichidae is often divided into two groups based primarily on morphological and morphogenetic characteristics, namely, the "flexible" non-stylonychine Oxytrichidae and the "rigid" Stylonychinae (Berger and Foissner, 1997; Berger, 1999). Bernhard et al. (2001) provided molecular evidence for the monophyly of Stylonychinae, which is not supported by further analyses (Foissner et al., 2004; Schmidt et al., 2007) and this study. The grouping of *Hemiurosomoida tibetensis* sp. nov. with its congeners corroborates the generic assignment of the species. The clustering of *Parakahliella macrostoma* into *Hemiurosomoida* clade suggests that the *Hemiurosomoida* is non-monophyletic (Chen et al., 2021). The first grouping of *P. macrostoma* with *H. warreni* corresponds to some morphological similarities (e.g., dorsal ciliary pattern and multiple macronuclear nodules) (Ning et al., 2018; Chen et al., 2021).

The present isolate of *Euplotes euryhalinus* first forms a clade with three populations of this species (EF094967, KP297368, MW369533), all sampled from same Antarctica as the original population and differing by 0–2 nucleotides from our population, which confirms our morphological identification. However, the Indian population with two sequences (JF903799, JF903800) shows (28, 44 different nucleotides, respectively) from our Chinese population, such great genetic divergence in SSU rRNA gene, which may infer that their species entities need reconfirmation as morphological data are unavailable for it. *Euplotes indica* and *E. magnicirratus* are within the clade of *Euplotes euryhalinus*, and this phylogenetic grouping is in accordance with some morphological similarities among these isolates, such as (1) C-shaped macronucleus and one spherical micronucleus; (2) ten frontoventral, five transverse, two left marginal, and two caudal cirri; (3) dorsal silverline system of double-*eurystomus* type, but *Euplotes euryhalinus* morphologically differs from *E. indica* by its larger ratio of buccal field length to body length (75 vs. 68%), more dorsal kineties (10 or 11 vs. 7), and different habitat (saline water vs. freshwater), from *Euplotes magnicirratus* by more dorsal kineties (10 or 11 vs. 8) and less dorsal ridges (6 vs. 8) (Gelei and Szabados, 1950; Carter, 1972; Valbonesi and Luporini, 1990; Abraham et al., 2021).

DATA AVAILABILITY STATEMENT

The datasets presented in this study can be found in online repositories. The names of the repository/repositories and accession number(s) can be found below: NCBI (accession: MZ457562, MZ457561); ZooBank (Present work: urn:lsid:zoobank.org:pub:C13AC67A-2F47-4879-9D90-3E45F67D33C6; Hemiurosomoida tibetensis sp. nov.: urn:lsid:zoobank.org:act:19F9C547-51C8-4F0C-83C9-9681ACBF0EC7).

AUTHOR CONTRIBUTIONS

XH designed the study. FK and WS identified species and drafted the manuscript. LJ and WZ performed the experiments and

constructed molecular trees. CW and TW analyzed data and made figures. All authors contributed to the proofreading of the manuscript and approved the final version.

FUNDING

This study was supported by the National Natural Science Foundation of China (project number: 41976086) and the China Scholarship Council, both awarded to XH.

ACKNOWLEDGMENTS

We thank Weibo Song, the Ocean University of China, for his long-term support and concern for the FK.

SUPPLEMENTARY MATERIAL

The Supplementary Material for this article can be found online at: https://www.frontiersin.org/articles/10.3389/fmars.2022.836341/full#supplementary-material

REFERENCES

Abraham, J. S., Somasundaram, S., Maurya, S., Gupta, R., and Toteja, R. (2021). Characterization of *Euplotes lynni* nov. spec., *E. indica* nov. spec. and description of *E. aediculatus* and *E. woodruffi* (*Ciliophora*, *Euplotidae*) using an integrative approach. *Eur. J. Protistol.* 79:125779. doi: 10.1016/j.ejop.2021.125779

Agatha, S., Spindler, M., and Wilbert, N. (1993). Ciliated protozoa (Ciliophora) from Arctic sea ice. *Acta Protozool.* 32, 261–268. doi: 10.1002/abio.370130414

Berger, H. (1999). Monograph of the Oxytrichidae (Ciliophora, Hypotrichia). *Monogr. Biol.* 78, 1–1080. doi: 10.1007/978-94-011-4637-1

Berger, H. (2001). *Catalogue of Ciliate Names: 1. Hypotrichs*. Salzburg: Verlag Helmut Berger.

Berger, H. (2006). Monograph of the Urostyloidea (Ciliophora, Hypotricha). *Monogr. Biol.* 85, 1–1304. doi: 10.1007/1-4020-5273-1_1

Berger, H. (2008). Monograph of the Amphisiellidae and Trachelostylidae (Ciliophora, Hypotricha). *Monogr. Biol.* 88, 1–737. doi: 10.1007/978-1-4020-8917-6

Berger, H. (2011). Monograph of the Gonostomatidae and Kahliellidae (Ciliophora, Hypotricha). *Monogr. Biol.* 90, 1–740. doi: 10.1007/978-94-007-0455-8

Berger, H., and Foissner, W. (1997). Cladistic relationships and generic characterization of oxytrichid hypotrichs (Protozoa, Ciliophora). *Arch. Protistenkd.* 148, 125–155. doi: 10.1016/S0003-9365(97)80048-6

Bernhard, D., Stechmann, A., Foissner, W., Ammermann, D., Hehn, M., and Schlegel, M. (2001). Phylogenetic relationships within the class Spirotrichea (Ciliophora) inferred from small subunit rRNA gene sequences. *Mol. Phylogenet. Evol.* 21, 86–92. doi: 10.1006/mpev.2001.0997

Borror, A. C. (1972). Revision of the order Hypotrichida (Ciliophora, Protozoa). *J. Protozool.* 19, 1–23. doi: 10.1111/j.1550-7408.1972.tb03407.x

Burkovsky, I. V. (1970). The ciliates of the mesopsammon of the Kandalaksha Gulf (White Sea) II. *Acta Protozool.* 7, 47–65.

Carey, P. G. (1992). *Marine Interstitial Ciliates: An Illustrated Key*. London: Chapman and Hall.

Carter, H. P. (1972). Infraciliature of eleven species of the genus *Euplotes*. *Trans. Am. Microsc. Soc.* 91, 466–492.

Chen, L., Liu, Y., Long, Y., Lyu, J., Feng, C., Ning, Y., et al. (2021). Morphology and molecular phylogeny of two new soil ciliates, *Hemiurosomoida warreni* nov. spec. and *Hemiurosoma clampi* nov. spec. (Ciliophora, Hypotrichia) from Tibet. *Eur. J. Protistol.* 77:125746. doi: 10.1016/j.ejop.2020.125746

Chen, X., Yan, Z., Al-Farraj, S. A., Al-Quraishy, S. A., El-Serehy, H. A., Chen, S., et al. (2013). Taxonomic descriptions of two marine ciliates, *Euplotes dammamensis* n. sp. and *Euplotes balteatus* (Dujardin, 1841) Kahl, 1932 (Ciliophora, Spirotrichea, Euplotida), collected from the Arabian Gulf, Saudi Arabia. *Acta Protozool.* 52, 73–89.

Curds, C. R. (1975). A guide to the species of the genus *Euplotes* (Hypotrichida, Ciliatea). *Bull. Br. Mus. Nat. Hist.* 28, 1–61.

Dragesco, J., and Dragesco-Kernéis, A. (1986). Ciliés libres de l'Afrique intertropicale. Introduction à la connaissance et à l' étude des Ciliés. *Faune Trop.* 24, 1–559.

Foissner, W. (2012). *Schmidingerothrix extraordinaria* nov. gen., nov. spec., a secondarily oligomerized hypotrich (Ciliophora, Hypotricha, Schmidingerotrichidae nov. fam.) from hypersaline soils of Africa. *Eur. J. Protistol.* 48, 237–251. doi: 10.1016/j.ejop.2011.11.003

Foissner, W. (2014). An update of 'basic light and scanning electron microscopic methods for taxonomic studies of ciliated protozoa'. *Int. J. Syst. Evol. Microbiol.* 64, 271–292. doi: 10.1099/ijs.0.057893-0

Foissner, W. (2016). Terrestrial and semiterrestrial ciliates (Protozoa, Ciliophora) from Venezuela and Galápagos. *Denisia* 35, 1–912.

Foissner, W., Staay, M., Staay, G., Hackstein, J., Krautgartner, W. D., and Berger, H. (2004). Reconciling classical and molecular phylogenies in the stichotrichines (Ciliophora, Spirotrichea), including new sequences from some rare species. *Eur. J. Protistol.* 40, 265–281. doi: 10.1016/j.ejop.2004.05.004

Fotedar, R., Stoeck, T., Filker, S., Fell, J. W., Agatha, S., Marri, M. A., et al. (2016). Description of the halophile *Euplotes qatarensis* nov. spec. (Ciliophora, Spirotrichea) isolated from the hypersaline Khor Al-Adaid lagoon in Qatar. *J. Eukaryot. Microbiol.* 63, 578–590. doi: 10.1111/jeu.12305

Ganner, B., Foissner, W., and Adam, H. (1986). Species separation in hypotrichous ciliates by classical morphological methods. *J. Protozool.* 135, doi: 10.1073/pnas.89.20.9764

Ganner, B., Foissner, W., and Adam, H. (1987). Morphogenetic and biometric comparison of four populations of *Urosomoida agiliformis* (Ciliophora, Hypotrichida). *Ann. Sci. Nat. Zool. Paris* 8, 199–207.

Gelei, J., and Szabados, M. (1950). Tömegprodukció városi esövizpoc-solyában (Massenproduktion in einer städtischen Regen-wasserpfütze). *Ann. biol. Univ. Szeged.* 1, 249–294.

Gong, R., Jiang, Y., Vallesi, A., Gao, Y., and Gao, F. (2020). Conjugation in *Euplotes raikovi* (Protista, Ciliophora): New insights into nuclear events and macronuclear development from micronucleate and amicronucleate cells. *Microorganisms* 8:162. doi: 10.3390/microorganisms8020162

Hall, T. A. (1999). BioEdit: a user-friendly biological sequence alignment editor and analysis program for Windows 95/98/NT. *Nucleic Acids Symp. Ser.* 41, 95–98.

Hu, X. (2014). Ciliates in extreme environments. *J. Eukaryot. Microbiol.* 61, 410–418. doi: 10.1111/jeu.12120

Hu, X., and Kusuoka, Y. (2015). Two oxytrichids from the ancient Lake Biwa, Japan, with notes on morphogenesis of *Notohymena australis* (Ciliophora, Sporadotrichida). *Acta Protozool.* 54, 107–122. doi: 10.4467/16890027AP.15.009.2734

Hu, X., Lin, X., and Song, W. (2019). *Ciliate Atlas: Species Found in the South China Sea*. Beijing: Science Press.

Ivalji, S., Scherwass, A., Schoenle, A., Hohlfeld, M., and Arndt, H. (2020). A barotolerant ciliate isolated from the abyssal deep sea of the North Atlantic: *Euplotes dominicanus* sp. n. (Ciliophora, Euplotia). *Eur. J. Protistol.* 73:125664. doi: 10.1016/j.ejop.2019.125664

Jankowski, A. W. (1979). Revision of the order Hypotrichida Stein, 1859. Generic catalogue, phylogeny, taxonomy. *Trudy Zool. Inst. Akad. Nauk. SSSR* 86, 46–85.

Jiang, J., Zhang, Q., Hu, X., Shao, C., Al-Rasheid, K. A. S., and Song, W. (2010a). Two new marine ciliates, *Euplotes sinicus* sp. nov. and *Euplotes parabalteatus* sp. nov., and a new small subunit rRNA gene sequence of *Euplotes rariseta* (Ciliophora, Spirotrichea, Euplotida). *Int. J. Syst. Evol. Microbiol.* 60, 1241–1251. doi: 10.1099/ijs.0.012120-0

Jiang, J., Zhang, Q., Warren, A., Al-Rasheid, K., and Song, W. (2010b). Morphology and SSU rRNA gene-based phylogeny of two marine *Euplotes* species, *E. orientalis* spec. nov. and *E. raikovi* Agamaliev, 1966 (Ciliophora, Euplotida). *Eur. J. Protistol.* 46, 121–132. doi: 10.1016/j.ejop.2009.11.003

Jung, J. H., Park, K. M., and Min, G. S. (2017). Morphology and molecular phylogeny of *Pseudocyrtohymenides lacunae* nov. gen., nov. spec. (Ciliophora: oxytrichidae) from South Korea. *Acta Protozool.* 56, 9–16. doi: 10.4467/16890027AP.17.002.6966

Kabir, A. S., Bharti, D., Kumar, S., Shazib, S. U. A., and Shin, M. K. (2020). Redescription of *Rigidohymena inquieta* (Stokes, 1887) Berger, 2011 as *Metahymena inquieta* gen. nov., comb. nov. (Ciliophora, Hypotricha) based on morphology, morphogenesis, and molecular phylogeny. *J. Eukaryot. Microbiol.* 67, 541–554. doi: 10.1111/jeu.12801

Kahl, A. (1930–1935). Urtiere oder *Protozoa*. I. Wimpertiere oder Ciliata (Infusoria), eine Bearbeitung der freilebenden und ectocommensalen Infusorien der Erde, unter Ausschlub der marinen Tintinnidae. *Tierwelt Dtl.* 25, 1–886.

Kaur, H., Shashi, P., Negi, R. K., and Kamra, K. (2019). Morphological and molecular characterization of *Neogastrostyla aqua* nov. gen., nov. spec. (Ciliophora, Hypotrichia) from River Yamuna, Delhi; comparison with *Gastrostyla*-like genera. *Eur. J. Protistol.* 68, 68–79. doi: 10.1016/j.ejop.2019.01.002

Kouris, A., Kim Juniper, S., Frébourg, G., and Gaill, F. (2007). Protozoan-bacterial symbiosis in a deep-sea hydrothermal vent folliculinid ciliate (*Folliculinopsis* sp.) from the Juan de Fuca Ridge. *Mol. Biol. Evol.* 28, 63–71. doi: 10.1111/j.1439-0485.2006.00118.x

Kumar, S., Bharti, D., Marinsalti, S., Insom, E., and Terza, A. L. (2014). Morphology, morphogenesis, and molecular phylogeny of *Paraparentocirrus sibillinensis* n. gen., n. sp., a "Stylonychine Oxytrichidae" (Ciliophora, Hypotrichida) without transverse cirri. *J. Eukaryot. Microbiol.* 61, 247–259. doi: 10.1111/jeu.12103

Kumar, S., Bharti, D., Shazib, S. U. A., and Shin, M. K. (2017). Discovery of a new hypotrich ciliate from petroleum contaminated soil. *PLoS One* 12:e0178657. doi: 10.1371/journal.pone.0178657

Kumar, S., and Foissner, W. (2017). Morphology and ontogenesis of *Stylonychia* (*Metastylonychia*) *nodulinucleata* nov. subgen. (Ciliophora, Hypotricha) from Australia. *Eur. J. Protistol.* 57, 61–72. doi: 10.1016/j.ejop.2016.09.001

Kumar, S., Stecher, G., and Tamura, K. (2016). MEGA7: molecular evolutionary genetics analysis version 7.0 for bigger datasets. *Mol. Biol. Evol.* 33, 1870–1874. doi: 10.1093/molbev/msw054

Küppers, G. C., Paiva, T. D. S., Borges, B. D. N., Harada, M. L., Garraza, G. G., and Mataloni, G. (2011). An Antarctic hypotrichous ciliate, *Parasterkiella thompsoni* (Foissner) nov. gen., nov. comb., recorded in Argentinean peat-bogs: morphology, morphogenesis, and molecular phylogeny. *Eur. J. Protistol.* 47, 103–123. doi: 10.1016/j.ejop.2011.01.002

Li, F., Li, Y., Luo, D., Miao, M., and Shao, C. (2018). Morphology, morphogenesis, and molecular phylogeny of a new soil ciliate, *Sterkiella multicirrata* sp. nov. (Ciliophora, Hypotrichia) from China. *J. Eukaryot. Microbiol.* 65, 627–636. doi: 10.1111/jeu.12508

Li, S., Bourland, W. A., Al-Farraj, S. A., Li, L., and Hu, X. (2017). Description of two species of caenomorphid ciliates (Ciliophora, Armophorea): morphology and molecular phylogeny. *Eur. J. Protistol.* 61, 29–40. doi: 10.1016/j.ejop.2017.08.001

Li, S., Zhuang, W., Pérez-Uz, B., Zhang, Q., and Hu, X. (2021). Two anaerobic ciliates (Ciliophora, Armophorea) from China: morphology and SSU rDNA sequence, with report of a new species, *Metopus paravestitus* nov. spec. *J. Eukaryot. Microbiol.* 68:e12822. doi: 10.1111/jeu.12822

Lian, C., Wang, Y., Jiang, J., Yuan, Q., and Shao, C. (2021). Systematic positions and taxonomy of two new ciliates found in China: *Euplotes tuffraui* sp. nov. and *E. shii* sp. nov. (Alveolata, Ciliophora, Euplotida). *Syst. Biodivers.* 19, 359–374. doi: 10.1080/14772000.2020.1865472

Lian, C., Wang, Y., Li, L., Al-Rasheid, K. A. S., Jiang, J., and Song, W. (2020). Taxonomy and SSU rDNA-based phylogeny of three new *Euplotes* species (Protozoa, Ciliophora) from China seas. *J. King Saud Univ. Sci.* 32, 1286–1292. doi: 10.1016/j.jksus.2019.11.013

Liu, W., Shin, M. K., Yi, Z., and Tan, Y. (2021). Progress in studies on the diversity and distribution of planktonic ciliates (Protista, Ciliophora) in the South China Sea. *Mar. Life Sci. Technol.* 3, 28–43. doi: 10.1007/s42995-020-00070-y

Luo, X., Huang, J., Bourland, W. A., El-Serehy, H. A., Al-Farraj, S. A., Chen, X., et al. (2021). Taxonomy of three oxytrichids (Protozoa, Ciliophora, Hypotrichia), with establishment of the new species *Rubrioxytricha guangzhouensis* spec. nov. *Front. Mar. Sci.* 7:623436. doi: 10.3389/fmars.2020.623436

Medlin, L., Elwood, H. J., Stickel, S., and Sogin, M. L. (1988). The characterization of enzymatically amplified eukaryotic 16S-like rRNA-coding regions. *Gene* 71, 491–499. doi: 10.1016/0378-1119(88)90066-2

Ning, Y., Yang, Y., Zhang, T., Chen, L., and Yi, Z. (2018). Integrative studies on the morphology, morphogenesis and molecular phylogeny of a soil ciliate, *Parakahliella macrostoma* (Foissner, 1982) Berger et al., 1985 (Ciliophora, Hypotrichia). *Acta Protozool.* 57, 107–122. doi: 10.4467/16890027AP.18.010.8984

Nylander, J. A. A. (2004). *MrModeltest version 2.1*. Uppsala: Evolutionary Biology Centre, Uppsala University.

Odhiambo, O. G., Wamalwa, Y. A., Omondi, O. S., Steffen, J., Michael, S., Bettina, S., et al. (2013). Ecology and community structure of ciliated protists in two alkaline–saline Rift Valley lakes in Kenya with special emphasis on *Frontonia*. *J. Plankton Res.* 35, 759–771. doi: 10.1093/plankt/fbt044

Oren, A. (2002). Diversity of halophilic microorganisms: environments, phylogeny, physiology, and applications. *J. Ind. Microbiol. Biotechnol.* 28, 56–63. doi: 10.1038/sj/jim/7000176

Pan, Y., Li, L. Q., Shao, C., Hu, X. Z., Ma, H. G., Alrasheid, K. A. S., et al. (2012). Morphology and ontogenesis of a marine ciliate, *Euplotes balteatus* (Dujardin, 1841) Kahl, 1932 (Ciliophora, Euplotida) and definition of *Euplotes wilberti* nov. spec. *Acta Protozool.* 51, 29–38. doi: 10.4467/16890027AP.12.003.0386

Petz, W., Song, W., and Wilbert, N. (1995). Taxonomy and ecology of the ciliate fauna (Protozoa, Ciliophora) in the endopagial and pelagial of the Weddel Sea, Antarctica. *Stapfia* 40, 1–223.

Qu, Z., Groben, R., Marteinsson, V., Agatha, S., Filker, S., and Stoeck, T. (2018). Redescription of *Dexiotricha colpidiopsis* (Kahl, 1926) Jankowski, 1964 (Ciliophora, Oigohymenophorea) from a hot spring in Iceland with identification key for *Dexiotricha* species. *Acta Protozool.* 57, 95–106. doi: 10.4467/16890027AP.18.009.8983

Qu, Z., Weinisch, L., Fan, X., Katzenmeier, S., Stoeck, T., and Filker, S. (2020). Morphological, phylogenetic and ecophysiological characterization of a new ciliate, *Platynematum rossellomorai* n. sp. (Oligohymenophorea, Scuticociliatia), detected in a hypersaline pond on Mallorca, Spain. *Protist* 171:125751. doi: 10.1016/j.protis.2020.125751

Schmidt, S. L., Bernhard, D., Schlegel, M., and Foissner, W. (2007). Phylogeny of the Stichotrichia (Ciliophora; Spirotrichea) reconstructed with nuclear small subunit rRNA gene sequences: Discrepancies and accordances with morphological data. *J. Eukaryot. Microbiol.* 54, 201–209. doi: 10.1111/j.1550-7408.2007.00250.x

Shao, C., Hu, C., Fan, Y., Warren, A., and Lin, X. (2019). Morphology, morphogenesis and molecular phylogeny of a freshwater ciliate, *Monomicrocaryon euglenivorum euglenivorum* (Ciliophora, Oxytrichidae). *Eur. J. Protistol.* 68, 25–36. doi: 10.1016/j.ejop.2019.01.001

Shao, C., Lu, X., and Ma, H. (2015). A general overview of the typical 18 frontal-ventral-transverse cirri oxytrichidae s. l. genera (Ciliophora, Hypotrichia). *J. Ocean Univ. China* 14, 522–532. doi: 10.1007/s11802-015-2482-7

Shen, Y. (1983). "Aquatic Invertebrates of the Tibetan Plateau," in *Protozoa of the Tibetan Plateau*, eds X. Jiang, Y. Shen, and X. Gong (Beijing: Science Press), 39–334.

Shimodaira, H. (2002). An approximately unbiased test of phylogenetic tree selection. *Syst. Biol.* 51, 492–508. doi: 10.1080/10635150290069913

Shimodaira, H., and Hasegawa, M. (2001). CONSEL: for assessing the confidence of phylogenetic tree selection. *Bioinformatics* 17, 1246–1247. doi: 10.1093/bioinformatics/17.12.1246

Singh, J., and Kamra, K. (2013). *Paraurosomoida indiensis* gen. nov., sp. nov., an oxytrichid (Ciliophora, Hypotricha) from Kyongnosla Alpine Sanctuary, including note on non-oxytrichid Dorsomarginalia. *Eur. J. Protistol.* 49, 600–610. doi: 10.1016/j.ejop.2013.04.001

Singh, J., and Kamra, K. (2015). Molecular phylogeny of *Urosomoida agilis*, and new combinations: *hemiurosomoida longa* gen. nov., comb. nov., and *Heterourosomoida lanceolata* gen. nov., comb. nov. (ciliophora, hypotricha). *Eur. J. Protistol.* 51, 55–65. doi: 10.1016/j.ejop.2014.11.005

Small, E. B., and Lynn, D. H. (1985). "Phylum Ciliophora Doflein," in *An Illustrated Guide to the Protozoa*, eds J. J. Lee, S. H. Hutner, and E. C. Bovee (Lawrence, KS: Society of Protozoologists), 393–575.

Song, W., Warren, A., and Hu, X. (2009). *Free-living Ciliates in the Bohai and Yellow Seas, China*. Beijing: Science Press.

Song, W., and Wilbert, N. (2002). Faunistic studies on marine ciliates from the Antarctic benthic area, including descriptions of one epizoic form, 6 new species and, 2 new genera (Protozoa: ciliophora). *Acta Protozool.* 41, 23–61.

Song, W., Zhang, T., Zhang, X., Warren, A., Song, W., Zhao, Y., et al. (2021). Taxonomy, ontogenesis and evolutionary relationships of the algae-bearing ciliate *Bourlandella viridis* (Kahl, 1932) comb. nov., with establishment of a new genus and new family (Protista, Ciliophora, Hypotrichia). *Front. Microbiol.* 11:560915. doi: 10.3389/fmicb.2020.560915

Stamatakis, A. (2014). RAxML version 8: a tool for phylogenetic analysis and post-analysis of large phylogenies. *Bioinformatics* 30, 1312–1313. doi: 10.1093/bioinformatics/btu033

Syberg-Olsen, M., Irwin, N. A. T., Vannini, C., Erra, F., Giuseppe, G. D., Boscaro, V., et al. (2016). Biogeography and character evolution of the ciliate genus *Euplotes* (Spirotrichea, Euplotia), with description of *Euplotes curdsi* sp. nov. *PLoS One* 11:e0165442. doi: 10.1371/journal.pone.0165442

Tuffrau, M. (1960). Révision du genre *Euplotes*, fondée sur la comparaison des structures superficielles. *Hydrobiologia* 15, 1–77.

Valbonesi, A., and Luporini, P. (1990). Description of two new species of *Euplotes* and *Euplotes rasiseta* from Antarctica. *Polar Biol.* 11, 47–53. doi: 10.1007/BF00236521

Wang, C., Hu, Y., Warren, A., and Hu, X. (2021). Genetic diversity and phylogeny of the genus *Euplotes* (Protozoa, Ciliophora) revealed by the mitochondrial CO1 and nuclear ribosomal genes. *Microorganisms* 9:2204. doi: 10.3390/microorganisms9112204

Wilbert, N. (1975). Eine verbesserte Technik der Protargolimprägnation für Ciliaten. *Mikrokosmos* 64, 171–179.

Xu, W., Zhao, Y., Pan, B., Liu, Y., Li, Y., Bourland, W. A., et al. (2020). Morphology, morphogenesis, and phylogeny of *Urosoma caudata* (Ehrenberg, 1833) Berger, 1999 (Ciliophora, Hypotrichia) based on a chinese population. *J. Eukaryot. Microbiol.* 67, 76–85. doi: 10.1111/jeu.12756

Xu, Y., Shao, C., Fan, X., Warren, A., Al-Rasheid, K. A. S., Song, W., et al. (2016). New contributions to the biodiversity of ciliates (Ciliophora, Hypotrichia) from Antarctica, including a description of *Gastronauta multistriata* nov. spec. *Polar Biol.* 39, 1439–1453. doi: 10.1007/s00300-015-1869-7

Conflict of Interest: The authors declare that the research was conducted in the absence of any commercial or financial relationships that could be construed as a potential conflict of interest.

Publisher's Note: All claims expressed in this article are solely those of the authors and do not necessarily represent those of their affiliated organizations, or those of the publisher, the editors and the reviewers. Any product that may be evaluated in this article, or claim that may be made by its manufacturer, is not guaranteed or endorsed by the publisher.